Functional Nanoparticle-Augmented Surfactant Fluid for Enhanced Oil Recovery in Williston Basin

Quarterly Status Report
(for the period of November 1, 2018 through February 1, 2019)

Prepared for:

Karlene Fine
Brent Brannan

North Dakota Industrial Commission
State Capitol, 14th Floor
600 East Boulevard Avenue, Department 405
Bismarck, ND 58505-0840

Contract No.: G-041-081

Prepared by:
Hui Pu
Julia Zhao
Department of Petroleum Engineering
Department of Chemistry
University of North Dakota

Research Team Members:
Xun Zhong
Chuncheng Li
Shaojie Zhang
Xu Wu
Yanxia Zhou

January 28, 2019

Summary of Current Progress

During the past quarter, our primary goals were to test the oil recovery of polymer nanofluid by physical simulation and molecular dynamics simulation of the behavior of nanoparticles/ surfactant. Specifically, we synthesized polymer nanoparticles (NPs), test the surfactant-based nanofluid stability in high salinity brine, conducted the core flooding experiments on Berea core samples and molecular dynamics simulation of oil transport through nano pores and the behavior of NPs/surfactant at the oil/water interface and the IFT reduction.

We mainly focused on the following tasks:

1) Synthesis of polymer nanoparticles
2) Surfactant-based polymer nanofluid stability experiment
3) Core flooding experiment using polymer nanofluid
4) Molecular dynamics simulation of oil transport through nano pores
5) Molecular dynamics simulation of NPs/surfactant at the oil/water interface

Below are the detailed results on the tasks.

1. Synthesis of polymer nanoparticle

1.1 Introduction

The synthesis of polymer NPs was based on a nano-precipitation method, where conjugated polymers firstly dissolved in a “good” solvent are added to an excess of “poor” solvent under ultrasonic dispersion. In this study, the nanoparticle was made with PFBT and PSMA in THF solution.

1.2 Summary and discussion

Figure 1 shows the DLS (dynamic light scattering) and zeta potential distribution of the polymer nanoparticles in distilled water. The hydrodynamic diameter distribution of particle sizes was mostly between 15~25nm. The zeta potential was between -40~-35mv.

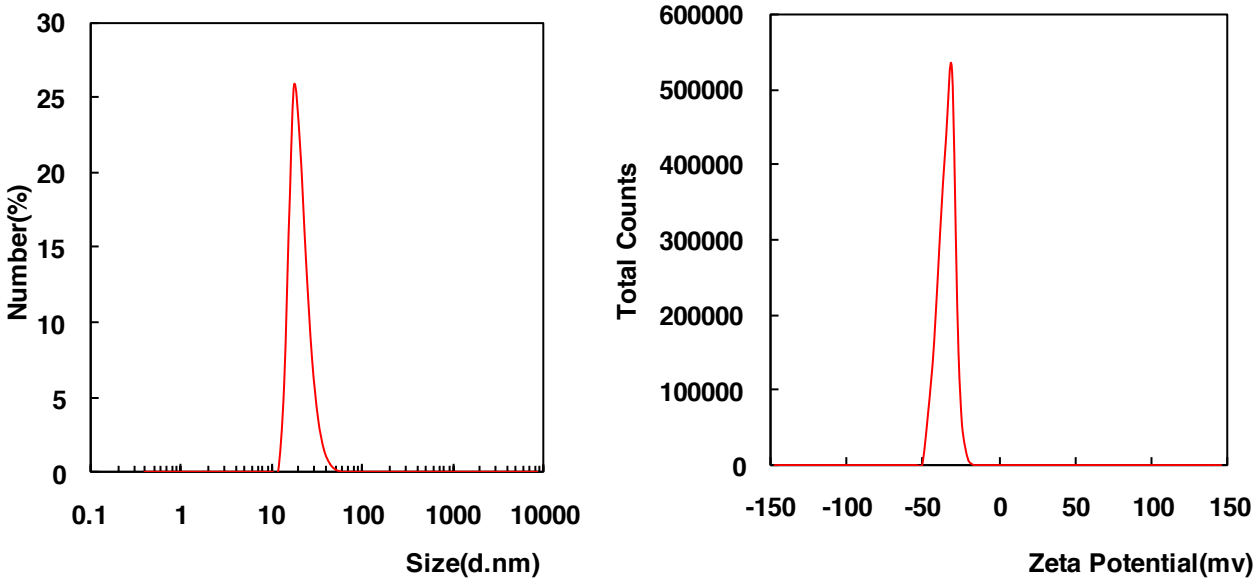

Figure1. DLS and zeta potential distribution of polymer nanoparticles

2. Stability test of surfactant-based polymer nanofluid

2.1 Introduction

The polymer nanofluid stability experiment was carried out at high salinity condition, the compositions of different salinity brines are shown in Table 1. Because the water-based polymer nanofluid was unstable under high salinity brine, the surfactant-based polymer nanofluid was prepared. Approximately 10 ml of the nanofluid samples were put in the oven at constant temperature of 80℃ over a 60-day period. DLS was used to measure the size distribution every 5 days.

Table1. Icon concentration of different salinity brines

Icon	Na^+	Ca^{2+}	Mg^{2+}	K^+	Cl^-	Total
mg/L	45639	8258.5	833.5	4340	91338	150409
	60845	11011	1111	5787	121783	200537
	76055	13765	1390	7235	152045	250490
	91278	16517	1667	8680	182676	300818

2.2 Summary and discussion

The surfactant-based polymer nanofluid is stable in all of the tested brines, including in 300,000 mg/L brine. Figure 2 shows the particle size results obtained from the stability experiment. Because the pore size of the Bakken formation is around 100nm, so in the follow up experiments, the 20wt% brine was chosen.

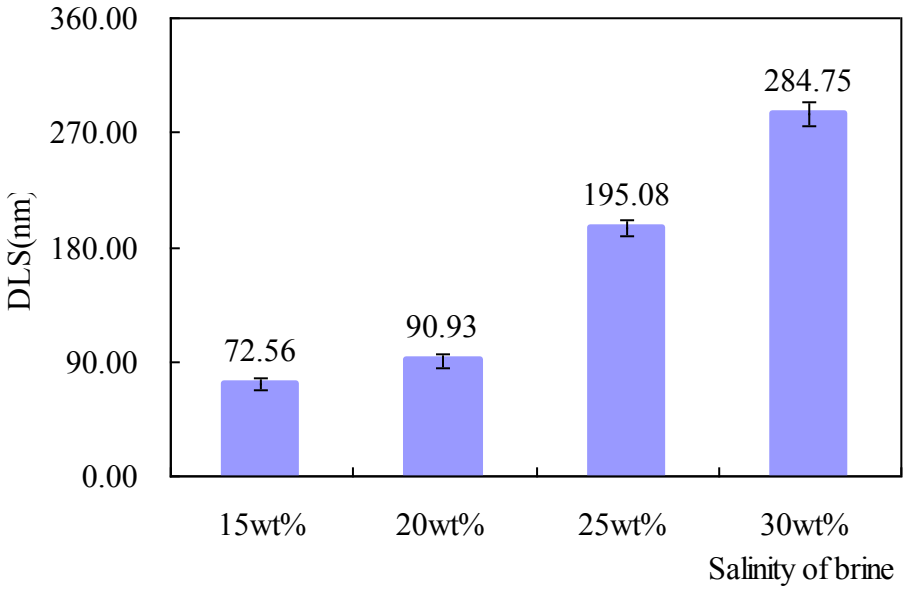

Figure2. DLS of polymer nanoparticles in different salinity brines

3. Core flooding experiment using polymer nanofluid

3.1 Introduction

In order to compare the oil recovery of surfactant solution and surfactant-based polymer nanofluid (SBPNF). Two types of oil displacement agents (surfactant solution, SBPNF) were tested for their ability to displace oil from core samples at 80℃ and the volumes of oil displaced from these cores were recorded with time.

3.2 Summary and discussions

Figure 3 shows the oil recovery profiles of surfactant flooding and surfactant-based nanofluid, both injected 0.5PV of solutions. It can be seen that comparing with brine flooding, surfactant flooding can enhance oil recovery by 7.91%OOIP, while surfactant-based nanofluid flooding yields an incremental oil recovery of 15.03%OOIP. These encouraging coreflooding results indicate that the incremental oil recovery by surfactant-based nanofluid flooding is 7.12%OOIP higher than that of surfactant flooding. Moreover, in the subsequent water flooding, the ultimate recovery from nanofluid-flooded sample is 1.44%OOIP higher than that of surfactant flooded core plug.

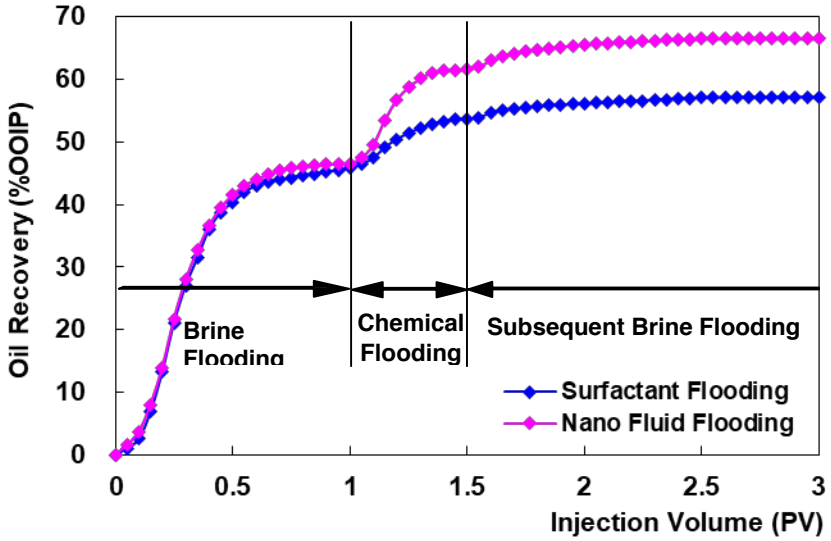

Figure 3. Oil recovery of surfactant flooding and surfactant-based nanofluid flooding

4. Molecular dynamics simulation of oil transport through nano pores

4.1 Introduction

The original wettability of rocks from Middle Bakken is oil- towards intermediate wet due to the mixture of water-wet inorganic pores and oil-wet organic pores. In the simulations, hydroxylated quartz and graphene are employed as water-wet and oil-wet rocks, separately. N-octane is used to represent oil because its properties are close to those of an oil mixture.

4.2 Summary

The transport behaviors of n-octane through quartz nano pore (Figure 4) and graphene nano pore (Figure 6) are studied by molecular dynamics simulation. The simulations are carried out at 383K, 35Mpa. The octane molecules lie dominantly parallel to the solid surface in the near-wall region. The mass density profiles (Figure 5, Figure 7) are symmetric with respect to the central plane (z=0) of the two rock surfaces. Dense octane layers exist in the near-wall region. From the spacing between two successive troughs, we determined the thickness of each monolayer (~0.45 nm). The density tends toward a constant (the bulk density at the same pressure and temperature) when it is farther away from the solid surface.

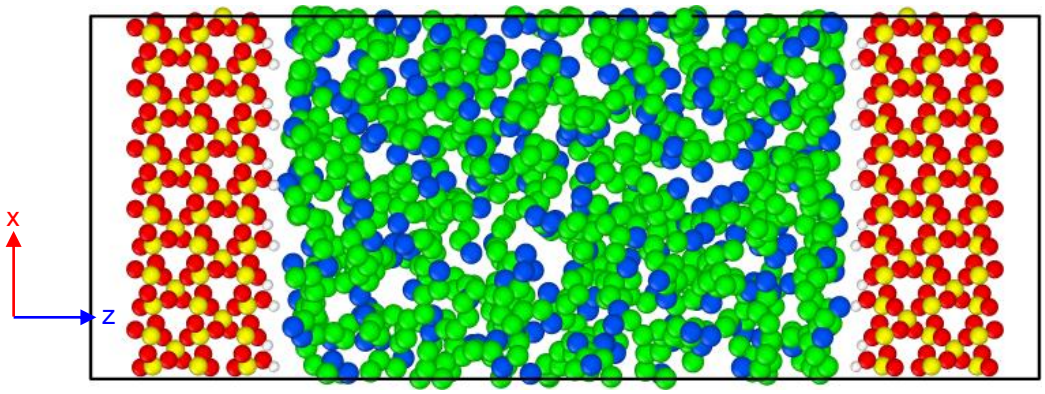

Figure 4. Simulation snapshot of n-octane flow through a 4.76nm hydroxylated quartz nanopore (Color code for atoms: red, oxygen; white, hydrogen; yellow, silicon; Blue and green, methyl (-CH_3) and methylene (-CH_2) groups in n-octane.

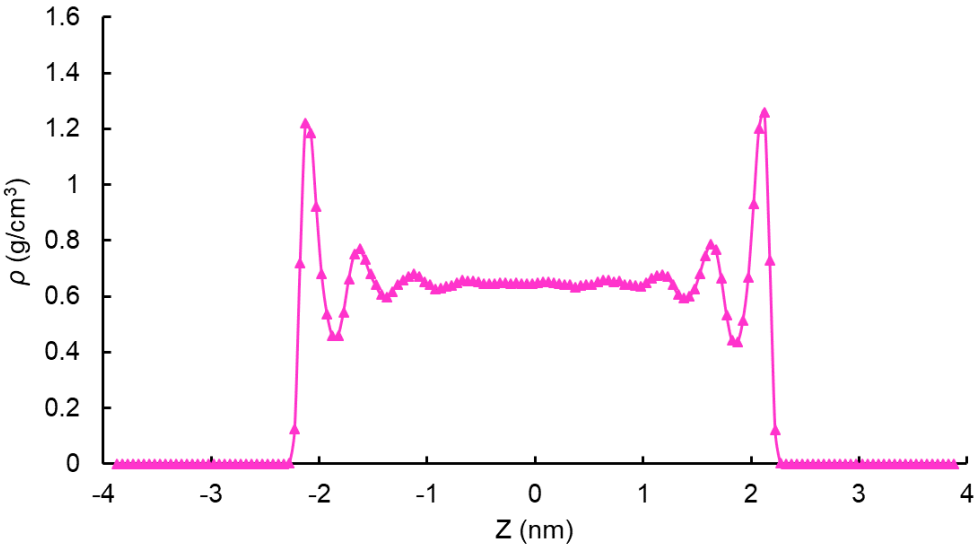

Figure 5. Mass density profile of n-octane confined in a 4.76nm quartz nanopore (383K, 35Mpa).

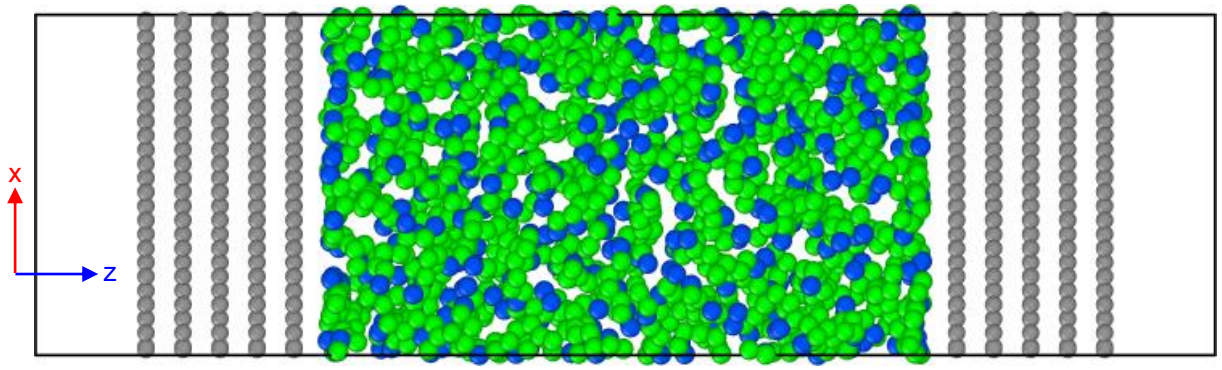

Figure 6. Simulation snapshot of n-octane flow through a 5.80 nm graphene nano pore (Color code for atoms: grey, carbon; Blue and green, methyl (-CH3) and methylene (-CH2) groups in n-octane.

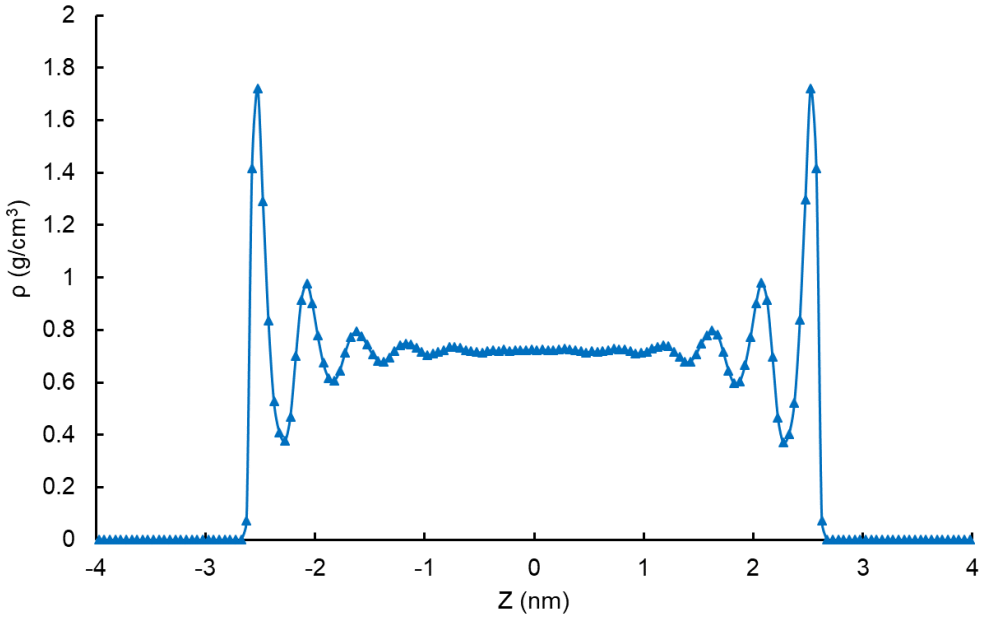

Figure 7. Mass density profile of n-octane confined in a 5.80 nm graphene nano pore (383K, 35Mpa).

By comparing the mass density profiles of n-octane confined in quartz and graphene nano pores, we can find that for each dense layer, the peak density of octane in graphene pores is much greater than that in quartz, indicating strong interactions and preferential adsorption of liquid hydrocarbons within carbonaceous material. In order to increase the mobility of oil in nano pores, it is crucial to alter core wettability from oil-wet to water-wet.

5. Molecular dynamics simulation of NPs/surfactant at the oil/water interface

5.1 Introduction

The laboratory experiments have been widely carried out to study the synergistic effect of NPs and surfactants on the enhanced oil recovery (EOR). In our work, molecular dynamics simulation is employed to study the behavior of NPs/surfactant at the oil/water interface and the IFT reduction. $C_{12}E_5$ and n-dodecane (C_{12}) are used to represent non-ionic surfactant and oil phase, respectively.

5.2 Summary

The IFTs of C_{12}/water and $C_{12}E_5/C_{12}$/water systems are calculated by molecular dynamics simulation (Figure 8). All simulations are carried out at 300 K and 1 atm. The IFT of C_{12}/water in our simulation is 51.30±0.18 mN/m which is in good agreement with the experimental value (52.8 mN/m). When the surfactant concentration is increased to an interfacial area of 56.25 $Å^2$ per $C_{12}E_5$, the IFT can be reduced to 22.10±0.18 mN/m.

NPs/$C_{12}E_5/C_{12}$/water systems (Figure 9) are also constructed to investigate the influence of various types of NPs on the ability of surfactants in term of interfacial tension (IFT) reduction. Figure 9 shows the distribution and organization of NPs and surfactants at the oil/water interface. The hydrophilic or hydrophobic NPs can only stay in a single phase. The hydrophilic or

hydrophobic NPs can hardly affect the IFTs. Amphiphilic NPs can stay at the oil/water interface and the IFT is reduced to 19.42±0.13mN/m.

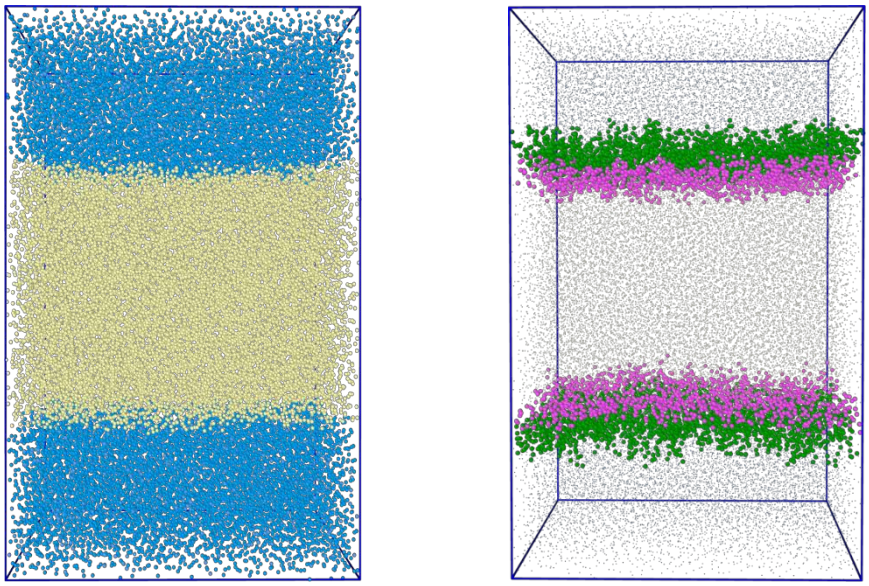

(a) (b)

Figure 8. Simulation snapshots of (a) C_{12}/water interface and (b) $C_{12}E_5$ in the vicinity of C_{12}/water interface (Color code for atoms: yellow, C_{12}; blue, water; pink, hydrophobic tail of $C_{12}E_5$; green, hydrophilic head of $C_{12}E_5$).

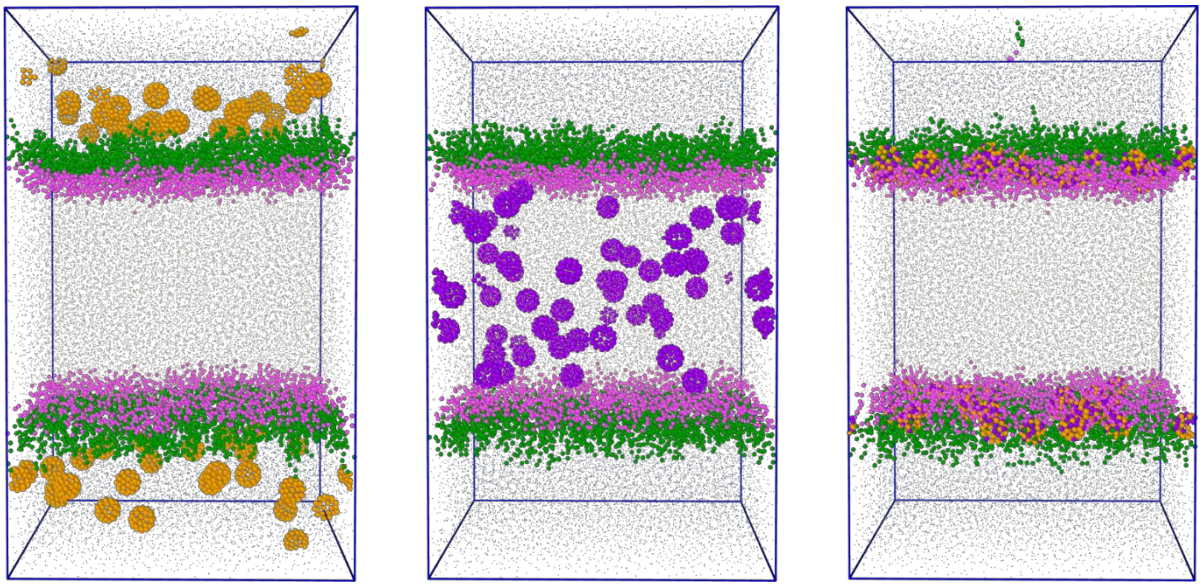

(a) (b) (c)

Figure 9. Simulation snapshots of NPs/$C_{12}E_5$ in the vicinity of C_{12}/water interface: (a) hydrophilic NPs, (b) hydrophobic NPs, (c) amphiphilic NPs. (Color code for atoms: gold, hydrophilic bead; purple, hydrophobic bead).

Figure 10 shows the organization of NPs and NPs/surfactants in the vicinity of the oil/water interface. Without surfactants, NPs tend to aggregate and form a big cluster. With surfactants added, the NPs are evenly distributed.

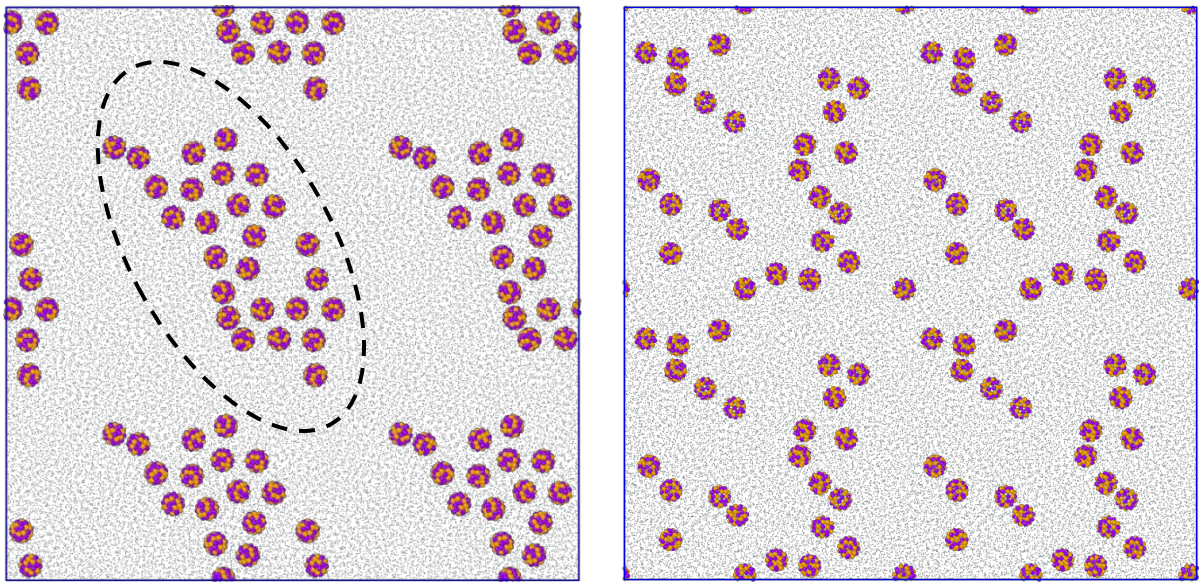

(a) (b)

Figure 10. MD simulation of (a) NPs and (b) NPs/surfactants ($C_{12}E_5$ molecules are omitted) in the vicinity of the C_{12}/water interface (top view).

Future Work

1. Synthesis of silicon quantum dots.
2. Water imbibition experiment using Bakken tight rocks.
3. Modification of nano fluid to enhance the temperature and salinity resistance.
4. The Influence of temperature, salinity, and surfactant type on the interfacial tension of the oil/water system.
5. Molecular dynamics simulation study on wettability alteration and oil detachment from oil-wet rock in aqueous surfactant solution
6. Molecular dynamics simulation study on oil detachment from different mineral surfaces in aqueous surfactant solution.